DOI:
10.1002/smll.201700147

Document Version
Publisher's PDF, also known as Version of record

The Nanomechanics of Lipid Multibilayer Stacks Exhibits Complex Dynamics

*Josep Relat-Goberna, Amy E. M. Beedle, and Sergi Garcia-Manyes**

The nanomechanics of lipid membranes regulates a large number of cellular functions. However, the molecular mechanisms underlying the plastic rupture of individual bilayers remain elusive. This study uses force clamp spectroscopy to capture the force-dependent dynamics of membrane failure on a model diphytanoylphosphatidylcholine multilayer stack, which is devoid of surface effects. The obtained kinetic measurements demonstrate that the rupture of an individual lipid bilayer, occurring in the bilayer parallel plane, is a stochastic process that follows a log-normal distribution, compatible with a pore formation mechanism. Furthermore, the vertical individual force-clamp trajectories, occurring in the bilayer orthogonal bilayer plane, reveal that rupturing process occurs through distinct intermediate mechanical transition states that can be ascribed to the fine chemical composition of the hydrated phospholipid moiety. Altogether, these results provide a first description of unanticipated complexity in the energy landscape governing the mechanically induced bilayer rupture process.

1. Introduction

The cell membrane, mainly composed of lipid moieties, is an extraordinary robust system that needs to preserve its physical integrity while withstanding chemical, electrical, and mechanical perturbations. The complexity of the lipid intermolecular forces endow membranes with the capability of undergoing the massive conformational changes required in endo- and exocytosis, membrane trafficking and cell division, while also regulating increasingly important mechanotransduction pathways.[1] In this context, pore formation is intricately linked to the mechanisms of cell fusion,[2] the formation of water and peptide-induced channels[3] and drug release.[4,5] Experimentally, pores can be typically created by electroporation[6] or through the application of mechanical forces (either by isotropic ultrasounds[7] or using, e.g., the pipette aspiration technique[8]). Despite important experimental and theoretical advances,[9] the precise molecular mechanisms underlying the formation of highly localized membrane transient rupture and their associated kinetics remains largely unknown.

The nanomechanics of lipid bilayers has been largely explored using atomic force microscope (AFM)-based force spectroscopy experiments, whereby the nanometer-sized cantilever tip applies an increasingly large force on a supported lipid bilayer until a discontinuity or "jump" is observed in the resulting force–distance curve, fingerprinting the rupture of the bilayer.[10] In these experiments, the vertical force applied to the bilayer is a direct measurement of the lateral interactions between phospholipid neighboring molecules.[11] The force value at which the discontinuity occurs, the "breakthrough force"(F_b), is regarded as the signature of the mechanical stability of the supported lipid bilayer.[12,13] From the theoretical perspective, such a membrane failure process has been typically interpreted as a simple barrier-limited, all-or-none reaction, whereby the height of the energy barrier (i.e., the bilayer survival probability) can be modulated by the applied force.[14,15] Despite such important progress, an intrinsic limitation of these experiments is that they are

Dr. J. Relat-Goberna, A. E. M. Beedle,
Prof. S. Garcia-Manyes
Department of Physics and Randall Division of Cell and Molecular Biophysics
King's College London
Strand, London WC2R 2LS, UK
E-mail: sergi.garcia-manyes@kcl.ac.uk

DOI: 10.1002/smll.201700147

typically conducted on individual bilayers that are supported on stiff, rigid substrates.[16] In spite of the lack of definitive experimental quantitative evidence, it is believed that the supporting substrate might have an important impact on the membrane nanomechanics.[17] Pore-spanning experiments and polymer cushioned single bilayers have attempted to mitigate such substrate effect.[18,19] An alternative means relies on the use of a hydrated lipid multibilayer stack composed of a large number (spanning from ≈100–500) of individual lipid bilayers.[20] This novel experimental design was successfully used in pioneering studies aimed at measuring the distinct mechanical resistance of bilayer stacks when indented by tips of varying chemistry.[21,22] Crucially, the use of lipid stacked multibilayers provides a much closer description for the cellular organelles that are obviously not surface-supported, some of them composed of more than one individual membrane, such as mitochondria or the nuclear envelope.[23–25]

With punctual exceptions,[26] the great majority of force spectroscopy AFM studies have thus far relied on the use of the force extension operational mode, where the force applied to the lipid membrane is measured as a function of the distance between the tip and the sample. While providing sound nanomechanical information, in these experiments the measured force changes very rapidly over extremely short distances, precluding the fine characterization of the subtleties characterizing the underlying free energy landscape.[27] Moreover, in these experiments determination of the elastic properties of the system requires precise knowledge of the tip shape.

To circumvent this, the force-clamp technique, initially designed to study the mechanical unfolding of individual polyproteins,[27–31] emerged. These experiments, where the applied force is kept constant thanks to an active proportional, integral and derivative (PID) feedback, measure the length evolution of the studied system over time,[32] providing a direct means to quantify the underlying energy landscape that ultimately determines the membrane breakthrough process.[33]

Here we make use of force-clamp spectroscopy to directly capture the force-induced rupture of the individual lipid bilayers composing a hydrated large multibilayer phospholipid stack, occurring one at a time. These measurements enable us to measure the substrate-independent and force-dependent kinetics of phospholipid bilayer rupture, providing a sub(molecular) picture of the rupturing process. Altogether, the statistical analysis of our force-clamp data directly reveals signatures of unanticipated complexity in the bilayer rupture process, compatible with a multiplicative pore-expansion mechanism.

2. Results

Using a homemade AFM force-clamp spectrometer (**Figure 1**a), we measured individual force–distance trajectories on a hydrated multibilayer stack of the model archeal DPhPC (diphytanoylphosphatidylcholine) lipid, amply used in single channel electrical recordings due to its high membrane stability[34,35] under buffered saline conditions (200×10^{-3} M NaCl, HEPES 10×10^{-3} M, pH 7.4). A topological AFM image of the stacked bilayer approach is shown in Figure S1 (Supporting Information). The resulting force-extension trajectory (Figure 1b) exhibits a saw-tooth pattern behavior, where each force peak corresponds to the rupture of an individual lipid bilayer by the AFM tip as revealed by the measured distance between two consecutive peaks (≈5.07 ± 0.7 nm). The average rupture force corresponding to $n = 1590$ rupture events from $n = 87$ independent trajectories ($F_b = 35 \pm 4$ nN, Figure 1c) is largely independent of the thickness of the lipid stack (Figure S2, Supporting Information). Noteworthy, in these force-extension experiments the breakthrough of an individual lipid bilayer results in a finite storage of nondissipated energy by the cantilever tip, which will increase the force at which the following individual bilayer will break. Importantly, as the tip approaches the mica substrate a decrease in the mechanical stability is observed, defining the "substrate-interface" region. This surface effect is highlighted in Figure 1d, showing the average breakthrough force ($n = 4220$, red) as a function of substrate distance and its standard deviation (gray region), demonstrating that the decrease in the mechanical stability occurs at ≈150 nm from the supporting substrate, thus corresponding to ≈30 layers.

Surprisingly, the first layer (in contact with the mica substrate, inset in Figure 1b) exhibits a distinct mechanical stability with respect to the rest of the bulk layers. Similarly,

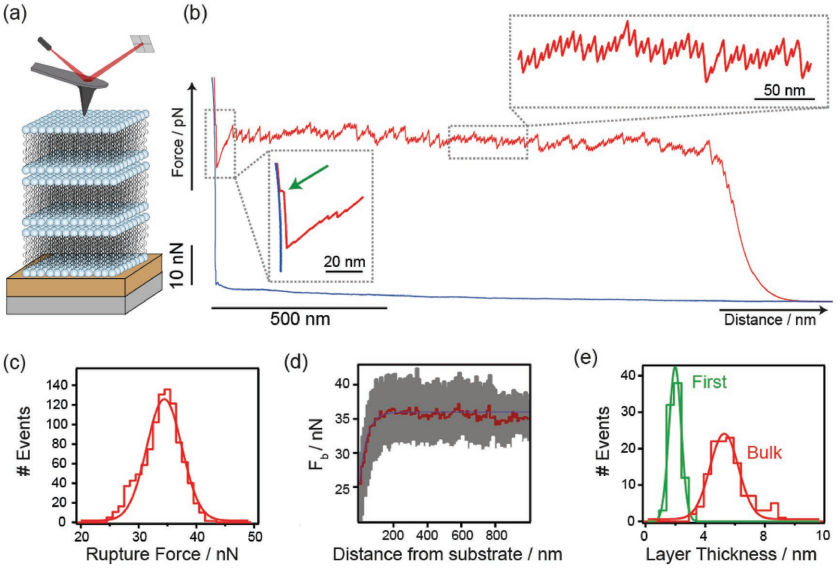

Figure 1. The rupture of a DPhPC stacked multilayer occurs through a layer-by-layer mechanism and it is affected by the supported substrate. a) Scheme of the AFM-based nanomechanical approach on a mica-supported multibilayer stack. b) The force versus distance plot exhibits a saw-tooth pattern, where each force-peak corresponds to the rupture event of an individual lipid bilayer. c) Each individual rupture event occurs at an average rupture force $F_b = 35 \pm 4$ nN, $n = 1590$. d) Deviation of the average force (red line) in the proximity of the mica support highlights a surface effect for the first ≈30 bilayers. e) The first bilayer in contact with the surface (a) inset) exhibits a much lower thickness ($\Delta d \approx 3.4$ nm) with respect to the rest of the bulk bilayers.

the thickness of such substrate-neighboring layer is dramatically smaller (down to ≈1.7 ± 0.6 nm) than the rest of the stacked membranes (≈5.1 ± 0.7 nm, Figure 1e). Hence, these nanomechanical experiments on multibilayer stacks demonstrate that, while only the first lipid bilayer in contact with the substrate is morphologically different from the rest, the mechanical effect of the substrate is much larger, encompassing up to ≈30 layers. The anomalous conformational and nanomechanical behavior of the first lipid bilayer in contact with the supporting substrate is also observed for multibilayers of lipids with distinct chemical composition, such as 1,2-dilauloyl-sn-glycero-3-phosphocholine (DLPC) and 1,2-dioleoyl-sn-glycero-3-phosphocoline (DOPC) (**Figure 2**).

Decoupling the mechanical effect originating from the supporting surface enables us to directly study the "unaffected" kinetics of membrane failure within the stacked multibilayer context. Applying a constant pushing force (force-clamp mode) of F = 30 nN to the DPhPC multibilayer sample (which minimizes the effect of the tip contact area) results in a linear decrease in the system length over time (**Figure 3**a). As expected, in the proximity of the supporting substrate, the AFM tip advances at a much increased velocity due to the mechanical destabilizing effect of the stiff substrate (purple area, "surface interface region"). Close inspection to the length–time indentation curve reveals that the trace is composed of individual steps (marked by a spike in the force channel) of 5.4 ± 0.3 nm (n = 130, Figure S3, Supporting Information) — a consistent value that lies in between the lamellar spacing determined by X-ray diffraction (D > 48 Å)[36] and the obtained by molecular dynamics simulations (D ≈ 60 Å)[34] — altogether demonstrating that the indentation of the multibilayer stack by the AFM tip occurs sequentially, one lipid bilayer at a time.

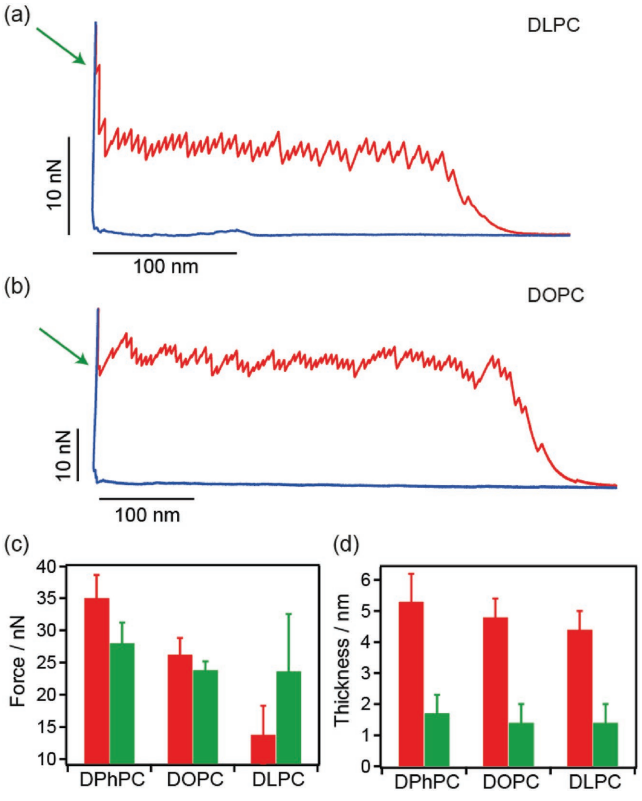

Figure 2. The mechanical effect of the supporting substrate is general and independent on the lipid chemistry. Individual indentation trajectories on a) DLPC and b) DOPC multibilayer stacks under constant velocity mode reveal that, similar to the trend observed for c) DPhPC the mechanical stability of the bilayer in contact with the mica supporting substrate (green) exhibits a mechanical stability that significantly differs from that obtained for the "bulk" bilayers (red). While in the case of DPhPC and DOPC the bilayer in close contact with the surface exhibits a lower mechanical stability than those present in the bulk, the situation is reversed for DLPC, where the inner bilayer displays a mechanical stability that is markedly higher than the rest of the stacked membranes. d) For all lipids, the thickness of the first membrane in contact with the substrate (green) is dramatically smaller than that corresponding to the bilayers forming the stack, probably due to a tilting effect. Altogether, these measurements demonstrate the anomalous mechanical and topological behavior of the first lipid bilayer in contact with the supporting mica substrate.

The rupture time between two consecutive steps (dwell time) hallmarks the mechanical stability of each bilayer. While the most intuitive scenario suggests a vertical hierarchy in the rupture process, whereby the top membrane breaks first and the rest follow subsequently until the substrate is reached, we cannot exclude the possibility that the applied pushing force might transmit to underlying membranes, allowing them to break before the upper one, to which the pushing force is directly applied. To check this hypothesis, we performed experiments (**Figure 4**a,b) on a lipid stack composed of a mixture of DOPC/sphingomyelin (SM)/cholesterol (Chol) (1:1:1), a model system forming two well-defined phases that align along the vertical direction[37] exhibiting markedly distinct mechanical properties.[38] Our force-extension (Figure 4c) and force-clamp (Figure 4d) individual indentation trajectories demonstrated that unlike in the stretching of polyproteins where unfolding follows a hierarchy in the mechanical stability,[39] the disruption of a poly lipid bilayer stack occurs according to the vertical physical order position of each bilayer, irrespective of its mechanical stability.

While the total time required to indent the whole DPhPC stack depends on its thickness (Figure 3b), a linear fit to the length versus time trace (which excludes the surface-interface region) yields in each case the rupture rate, which is independent of the stack thickness (R^2 = 0.0016, Figure 3b). In order to test whether the rupture of each individual DPhPC membrane composing the stack is an independent event, we analyzed the dwell time distribution corresponding to 152 individual indentation trajectories on different bilayer stacks at the same pushing constant force of 30 nN, and each penetration trajectory was individually reconstructed (Figure 3c). The autocorrelation function for each rupture event shows no significant correlation between two consecutive events (Figure 3d), thus demonstrating that the rupture dwell times from different trajectories can be safely pooled together to obtain an average indentation master curve at a given constant force. Most importantly, these results demonstrate, contrary to previous belief,[26] that stacked lipid bilayers behave like a chain of stochastic events, reminiscent of a Poisson process.

Using this statistical analysis, we studied the force dependency of the rupture kinetics of the stacked bilayers.

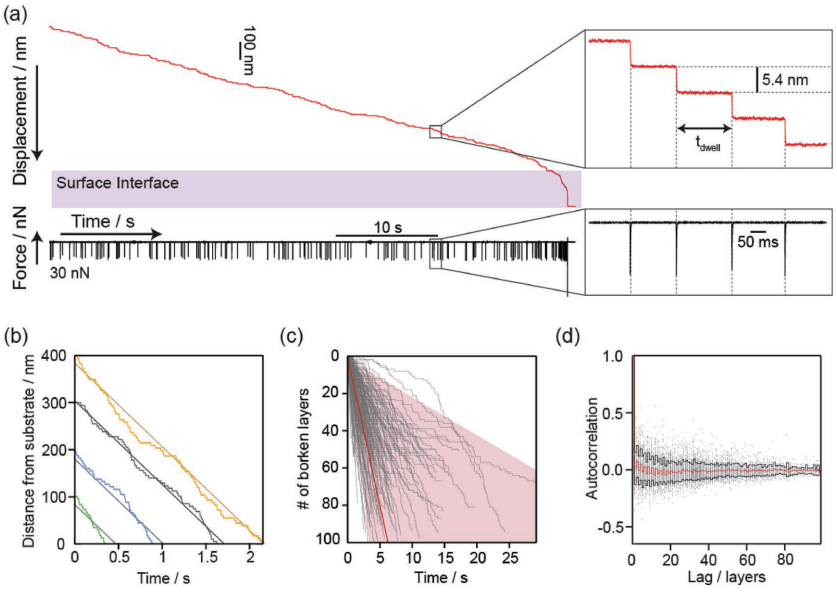

Figure 3. The rupture kinetics of the DPhPC multilayer is a step-by-step memory-less process as revealed by force-clamp AFM experiments. a) The linear force-clamp indentation trajectory on a stacked DPhPC multilayer recorded at a constant force of $F = 30$ nN is composed of individual steps of 5.4 ± 0.3 nm ($n = 130$), hallmarked by a spike in the force channel. The indented region close to the surface (purple box) exhibits a higher rupture rate. b) A linear fit to the indentation trajectories corresponding to four distinct stacks containing a different number of bilayers captures their associated rupture rate. c) Reconstruction of the time-course evolution of 152 indentation trajectories from their measured dwell times. The average rupture rate (16 ± 13 layers, solid red line) and its standard deviation (light red area) are represented. d) The autocorrelation function of the rupture times as a function of the number of layers (lag) shows no correlation between two consecutive events.

To this goal, we systematically changed the applied force applied to the DPhPC multilayer, spanning the range of forces 24–36 nN. As observed in **Figure 5**a, the bilayers break quicker as the force is increased. We measured the average rupture rate, α, (calculated as the inverse of the rupture time) and plotted the $\ln(\alpha)$ as a function of the applied force (Figure 5b). The exponential force dependency confirms that the rupture of stacked lipid membranes is a force-activated, barrier-crossing process. Experimental data was fitted to the Bell model:[40]

$$\alpha(F) \equiv \alpha(0) \exp\left(\frac{\Delta x}{N \cdot k_B T} F\right) \quad (1)$$

where $\alpha(0)$ is the rate in the absence of force, Δx is the distance to the transition state, and N, the number of disrupted interactions. Fitting the Bell equation to the experimental data yields $\ln[\alpha(0)] = -12.2 \pm 0.9$ and $\Delta x/N = 1.87 \pm 0.04$ pm. This value is similar to that obtained previously.[22,26] However, this latter term is devoid of physical meaning as long as $N \neq 1$. Unfortunately, unambiguous and quantitative description of N is experimentally challenging due to the uncertainty in the absolute determination of the small tip-surface contact area, likely influenced by the shape of the asperities of the indenter tip. In effect, the rupture of the lipid membrane involves the creation of a pore that allows the AFM tip to break through, concomitant to the cleavage of a number of lateral lipid–lipid interactions.[14] Indeed, electroporation studies suggest that metastable pre-pores can exist up to 10 nm of radius,[6] which corresponds to hundreds of lipid molecules. It is then possible that the creation of a stable pore (occurring in the plane perpendicular to the application of force) with a critical radius—similar to a nucleation process[41]—is the rate-limiting step for the membrane rupture. Hence, a molecular description in terms of the Bell formalism might be just not applicable since the position of the transition state, Δx, is likely to be placed on an orthogonal coordinate to the pushing force, namely that of the lipid–lipid interaction plane.

To by-pass the uncertainty in the determination of the critical radius, and in order to obtain further insight into the statistical details that characterize the rupture kinetics process beyond the Bell formalism, we analyzed the time distribution of rupture events occurring at $F = 30$ nN with a statistical pool of data as large as 9125 events. Surprisingly, instead of the expected exponential distribution evocative of a barrier-limited all-or-none process, the obtained distribution displays a right-skewed unimodal shape, with rupture events spanning several decades (from a few milliseconds all the way up to several seconds). To certify that the relative lack of short-time events is not a result of the limited-bandwidth of the (PID) feedback of our force-clamp spectrometer, we repeated the experiments at a lower force of $F = 26$ nN and observed the same nonexponential trend, ensuring that the observed distribution is an intrinsic property of the kinetics of rupture of the lipid membrane (Figure S4, Supporting Information). The representation of the probability density function (PDF) in terms of $\ln(t)$ follows a normal distribution (Figure 5d). Four different models that can account for the nonexponential distribution associated to a time-increasing hazard rate (namely log-normal,[42] inverse Gaussian,[43] Chizmadzhev and co-workers,[44,45] and Weibull[30,46] distributions) are fitted to the PDF. A description of all different models and their physical implications is included in Supporting Information. The log-normal distribution, which in the logarithmic space, $y = \ln(t)$, recovers the normal distribution (Figure 5d), fits the PDF function with the smallest error (Figure 5e). Log-normal distributions are characteristic of multiplicative growth processes, where the instantaneous growth is proportional to the current size of the system.[42] This is fully compatible with a pore growth mechanism,[41] (Figure 5f). According to this model, when a defect in the lipid membrane structure is created, expansion through the adjacent molecules will be more energetically favorable because the boundary lipids have a lower number of lipid neighbors to bind to. As more defects are created, the number of boundary lipids will increase proportionally to the effective perimeter of the pre-pore, hence generating

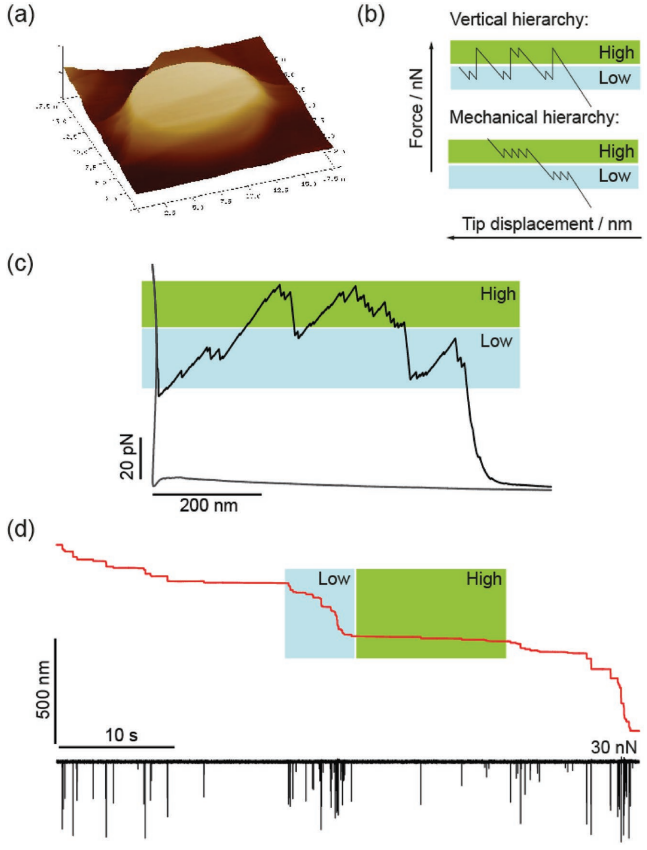

Figure 4. Stacked lipid membranes break following a vertical (and not a mechanical) hierarchy. a) Topography AFM image of a surface of a DOPC/sphingomyelin/cholesterol (1:1:1) mixture, which produces phase-segregated lipid stacks that align on the vertical direction. b) Schematic diagram of the expected force-extension profile in case the rupture process of a multibilayer sample with binary mechanical stability follows either a vertical (top) or mechanical (bottom) hierarchy. c) Constant velocity pushing experiments on the DOPC/sphingomyelin/cholesterol (1:1:1) stacked mixture yield force versus distance profiles with alternating high and low mechanical stability individual bilayers, corresponding to the indentation of the liquid-ordered and liquid-disordered phases, respectively. d) Analogous experiments under force-clamp conditions (F = 30 nN) reveal typical distance–time recordings whereby the fast steps (corresponding to low mechanical stability bilayers) alternate with slow steps (which fingerprint mechanically resistant ones), providing a nonlinear indentation trace. Altogether, these experiments demonstrate that, contrary to the mechanical stretching of individual polyprotein chains, which follows a hierarchy in the mechanical stability, the indentation of lipid multibilayer stacks simply follows a hierarchy in the vertical position.

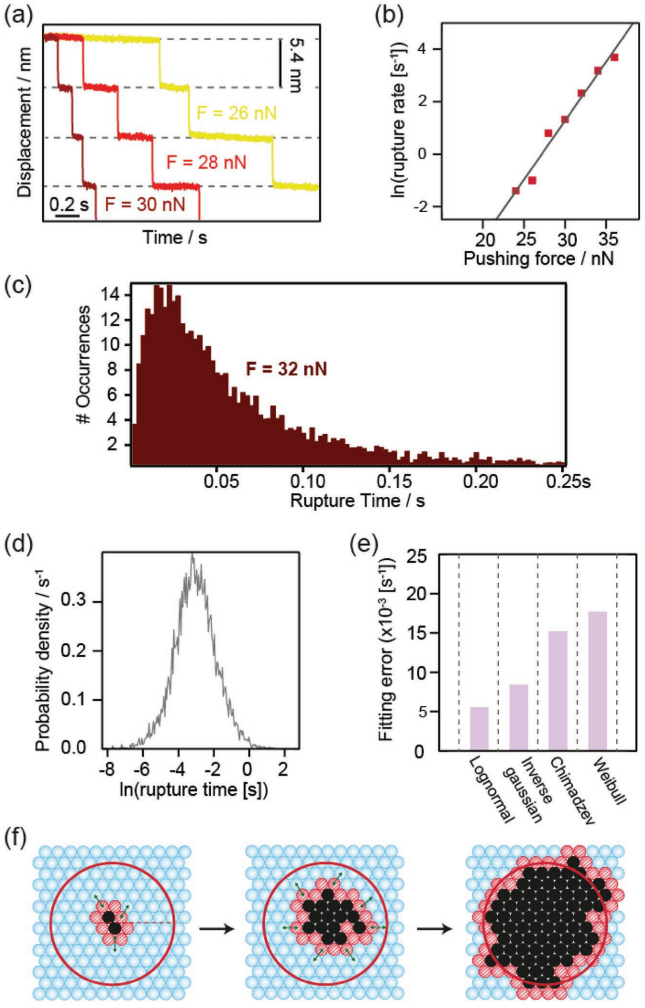

Figure 5. The distribution of rupture dwell-times can be best captured by a log-normal distribution. a) The time course of bilayer stack rupture decreases as the pushing force is increased. b) The inverse of the average rupture time yields the rupture time at each force (red dots). Fitting the Bell model yields $\Delta x/N$ = 1.87 ± 0.04 pm and $\ln[\alpha(0)] = -2.2 \pm 0.9$. c) The rupture time distribution at F = 32 nN exhibits a marked nonexponential behavior that follows d) a log-normal distribution with e) the smallest error fit. f) Schematic representation of the proposed model of pore growth lipid rupture model.

a multiplicative growth process. When a critical pore size is reached, the pore will become stable and the lipid membrane will rupture (Figure 5f). Crucially, while different values of the tip-surface contact area will change the mean time of lipid membrane rupture, they will not affect the log-normal distribution of rupture times. To further illustrate this argument, we developed a proof-of-concept stochastic simulation to model the multiplicative pore growth mechanism (Supporting Information). The resulting rupture time PDF retained the log-normal distribution (Figure S5, Supporting Information). The agreement between both time distributions strongly supports the multiplicative nature of rupture processes.

Further signatures of complexity can be also observed in the bilayer perpendicular plane, directly through the length–time indentation traces obtained with our force-clamp approach (**Figure 6**). So far the stacked lipid membranes were indented at relatively high pushing forces, allowing to measure their failing kinetics within experimentally affordable timescales (Figures 3 and 5). However, one of the advantages of the force-clamp technique lies in its capability to readily expand the time window of experimentation. Pushing the bilayer stack at relatively low forces slows down the rupture rate exponentially (Figure 5b), enabling to capture fine details of the rupture process that were invisible at high pushing forces and also when using classical constant velocity mode, reporting a simple transition between the unruptured to the ruptured lipid conformation. When a constant force as low as F = 22 nN (or ≈65% of the average membrane breakthrough force) is applied, in ≈30% of the occurrences

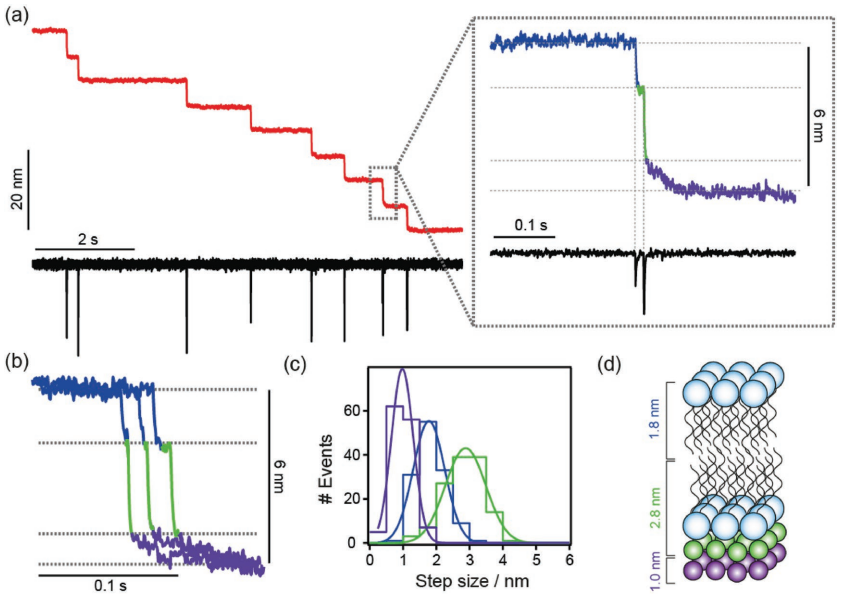

Figure 6. The vertical rupture of an individual bilayer occurs through multiple mechanical transition states. a) Indenting the multi bilayer stack at low forces reveals the presence of two mechanical intermediates b) occurring in consistent positions. c) The distribution of measured lengths for each intermediate is compatible with the d) fine chemical structure defining the hydrated DPhPC phospholipid chemical moiety.

the rupture of each individual DPhPC lipid membrane is no longer observed as a single transition (Figure 6a). Rather, analysis of $n = 353$ individual breakthrough events reveals that each ≈5 nm step is split into several smaller steps, which are also identified as clear spikes in the force channel (Figure 6a). While the number of substeps varies, the most frequently observed scenario involves the presence of three individual steps (Figure 6b), measuring $L_1 = 1.8 \pm 0.5$, $L_2 = 2.8 \pm 0.6$, and $L_3 = 1.0 \pm 0.3$ nm, respectively (Figure 6c), indicative of at least two distinct mechanical energy barriers. Notably, these lengths add up to the full length of ≈5.6 nm that characterizes the tip penetration of an individual lipid bilayer. In some other cases, probably due to limited time resolution, only two steps were captured, either in the order $L_1 + (L_2 + L_3)$ or $(L_1 + L_2) + L_3$, as shown in Figures S6 and S7 (Supporting Information), respectively.

While it is premature to unambiguously ascribe each particular step to the rupture of a defined region of the phospholipid moiety, the X-ray structure of hydrated DPhPC multibilayers[36] allows for an educated guess. In the absence of hydration, the peak-to-peak distance obtained from the electron density profiles along the bilayer normal is 37 Å,[36,47] entailing that each independent leaflet measures 3.7/2 = 1.85 nm. Thus, it is tempting to speculate that the first step (L_1) corresponds to the independent rupture of the first leaflet. In this vein, L_2 would correspond to the combined rupture of the second leaflet together with the first hydration layer. Noteworthy, both L_1 and L_2 steps occur within a timescale of ≈5 ms, readily measurable with our force-clamp approach. The remaining 1.0 ± 0.3 nm (L_3) step might fingerprint the rupture of the second layer of confined water,[34] occurring within timescales spanning from >5 ms all the way up to <500 ms (Figure S8, Supporting Information). Such much slower timescale is compatible with the slow, anomalous diffusion of confined water (in the presence of ionic strength) in a multilamellar bilayer,[48] probably due to a time-dependent diffusion coefficient.[49] Altogether, our indentation experiments highlight the presence of transient mechanical states that reveal the substructure of individual hydrated bilayers, suggesting that both lipids leaflets are mechanically independent, thus departing from the well-established all-or-none rupturing process.

3. Conclusions

Using a novel multibilayer stack approach that avoids the large mechanical effect of the stiff supporting substrate, our experiments using force-clamp spectroscopy provide direct evidence that the membrane rupture reaction occurs through a multistep process in two orthogonal planes. The measured fracture time distribution is reminiscent of a multiplicative growth process, which can be easily interpreted in the framework of a pore nucleation model, whereby a pore expands through its perimeter along the perpendicular direction to the applied force (and thus parallel to the bilayer) until an irreversible, critical size is reached.[50] In this scenario, the radius of the critical pore would become the real determinant of the kinetics of lipid rupture, suggesting that the critical radius is independent, and possibly larger, than the tip indenter. On the bilayer perpendicular plane, our force clamp experiments at low pushing forces identified at least two mechanically transient intermediate states occurring after the formation of the pore in the lipid membrane, which are compatible with the rupture of key substructural features within the phospholipid moieties. Altogether, our experimental observations with increased length, time, and force resolution, unveil new signatures of complexity that expands and challenge the currently accepted simplistic two-state model of lipid rupture. We anticipate that these experiments will open the door to the study of complex bilayer systems, formed by chemically distinct phospholipid entities with varying compositions,[12] and under distinct ionic strength conditions,[51–53] with the ultimate goal to eventually unveil the physicochemical and mechanical complexity that characterizes the plasma membrane.

4. Experimental Section

Lipid Multibilayer Sample Preparation: Hydrated stacked lipid membranes were formed following the procedure described by Tristram-Nagle.[54] In their method, the lipid membranes were directly formed on the substrate instead of deposited from liposome suspensions. First, the lipids (Avanti Polar Lipids, Alabaster, AL) were

dissolved in CH_3Cl/MeOH (3:1) (>99% purity from Sigma-Aldrich, Saint Louis, MO) to give a final concentration between $\approx 2 \times 10^{-3}$ and 20×10^{-3} M depending on the desired stack thickness. For the dual-phase stacked lipid experiments, a 1:1:1 DOPC/SM/Chol mixture was used. Then, a small aliquot (1–10 µL) was spread on top of a freshly cleaved Muscovite Mica substrate (Agar Scientific, Stansted, UK) and quickly dried under a gentle flow of nitrogen gas. Then, the nitrogen flow was maintained at lower pressures for 40 min to evaporate any remaining organic solvent traces. After evaporation, the dried lipids have already structured into stacked membranes. Our results are also in agreement with previous studies with dry DOPC lipid stacks.[20,55]

Working with the lipid stacks in aqueous environment proved to be more challenging. Hydrated stacked membranes have a great tendency to wash away or "peel off,"[56,57] especially in the case of thin (0.1–8 µm) lipid stacks. For this reason, lipid stacks are typically investigated in saturated humidity air environments where they cannot float in the aqueous medium.[54] Alternatively, very thick lipid stacks are employed when a larger number of stacked lipid membranes are required.[37,58] We investigated the suitable hydration condition for a strong substrate attachment. We discovered that mild temperatures and longer resting time favor the attachment of lipids to the substrate. In our protocol, the samples were heated at low temperature (‹50 °C) in buffer solution (200×10^{-3} M NaCl, HEPES 10×10^{-3} M, pH 7.4) for at least 2 h and then were left to settle overnight under saturating water conditions. During the experiments, the same buffer was kept without any rinsing to avoid the detachment of the lipid stacks due to turbulences. Even though this method still has a poor success rate (≈30%), it has allowed for the first time to study thin (<0.1–8 µm) liquid state lipid stacks.

Atomic Force Microscopy Force Measurements—Constant Velocity Experiments: The force versus distance plots were acquired by allowing the AFM tip approach the surface at a constant velocity (1000 nm s^{-1}) until the substrate was encountered and all the individual lipid bilayers within the stack were pierced. The AFM cantilever was first calibrated against a clean, freshly cleaved mica using the equipartition theorem.[59] An SNL-10 tip A (Bruker Probes, Karlsruhe, Germany) with a typical spring constant $k = 0.35$ N m^{-1} was used for all investigations. The AFM cantilevers were thoroughly rinsed and dried after calibration in order to avoid contamination. All experiments were performed at 22 °C in a temperature-controlled room with a stability of ±1 °C.

Atomic Force Microscopy Force Measurements—Force-Clamp-Experiments: Force-clamp AFM experiments were performed by applying a constant force between the AFM tip and the surface. An external feedback mechanism was used to maintain a constant AFM cantilever deflection (force) by controlling the position of the surface with a piezoelectric actuator. The feedback loop consisted of proportional, integral, and derivative terms (PID) and displayed a time response faster than 1 ms.[33] The unprecedented quick response of our feedback loop stems from the higher resonant frequency of the cantilevers used and the small distance (≈5 nm) that the piezoelectric actuator has to travel in order to recover the set-point deflection.

Data Analysis—Force-Clamp Analysis: Force-Clamp traces were analyzed using a specifically written software developed in our lab using Igor Pro (WaveMetrics, Portland, OR). In this software, the user manually spotted the lipid membrane rupture events and measured its rupture time and lipid membrane thickness by clicking on the curve. The measured values for each step were stored in a matrix containing all the rupture events from the same trajectory. Each matrix contained information on the date and time of the experiment and on the source trajectory. The matrix also allowed the user to assign a tag to the rupture event in order to analyze trajectories that display various substeps. The analysis results were automatically displayed on top of the original trace to allow later review. In all cases, the surface interface area was excluded from the analysis.

The rupture rate was measured using two independent procedures. In the first one, the average rupture rate was obtained from whole trajectories. In this case, the lipid membrane rupture times were used to reconstruct each individual force-clamp trajectory. Instead of using the original traces, calculating the reconstructed trajectories allowed to directly compute the rupture rate without accounting for the lipid membrane thickness. Each reconstructed trajectory was then fitted with a linear function and the slope was used to calculate the average rupture rate and the related standard deviation. In addition, the reconstructed traces were used to calculate the autocorrelation function. In the second procedure, each rupture time was computed as the dwell time between the current and previous rupture events. All dwell times were then pooled together and the inverse of the mean was taken as the rupture rate. This same procedure was used to calculate the rupture time distributions.

Supporting Information

Supporting Information is available from the Wiley Online Library or from the author.

Acknowledgements

J.R.-G. was recipient of a "La Caixa" fellowship. This work was supported by the Marie Curie CIG (293462) and BBSRC (J00992X/1) grants, and by the EPSRC Fellowship (K00641X/1), all to S.G.-M.

[1] A. E. Beedle, A. Williams, J. Relat-Goberna, S. Garcia-Manyes, *Curr. Opin. Chem. Biol.* **2015**, *29*, 87.
[2] L. V. Chernomordik, M. M. Kozlov, *Nat. Struct. Mol. Biol.* **2008**, *15*, 675.
[3] M. T. Lee, W. C. Hung, F. Y. Chen, H. W. Huang, *Proc. Natl. Acad. Sci. USA* **2008**, *105*, 5087.
[4] A. Delalande, M. Postema, N. Mignet, P. Midoux, C. Pichon, *Ther. Delivery* **2012**, *3*, 1199.
[5] L. Gibot, M. P. Rols, *Expert Opin. Biol. Ther.* **2016**, *16*, 67.
[6] J. C. Weaver, Y. A. Chizmadzhev, *Bioelectrochem. Bioenerg.* **1996**, *41*, 135.
[7] F. Padilla, R. Puts, L. Vico, K. Raum, *Ultrasonics* **2014**, *54*, 1125.
[8] W. Rawicz, K. C. Olbrich, T. McIntosh, D. Needham, E. Evans, *Biophys. J.* **2000**, *79*, 328.
[9] D. P. Tieleman, H. Leontiadou, A. E. Mark, S. J. Marrink, *J. Am. Chem. Soc.* **2003**, *125*, 6382.
[10] S. Garcia-Manyes, F. Sanz, *Biochim. Biophys. Acta* **2010**, *1798*, 741.

[11] Y. F. Dufrene, T. Boland, J. W. Schneider, W. R. Barger, G. U. Lee, *Faraday Discuss.* **1998**, *79*, Discussion 137.
[12] S. Garcia-Manyes, L. Redondo-Morata, G. Oncins, F. Sanz, *J. Am. Chem. Soc.* **2010**, *132*, 12874.
[13] S. Kunneke, D. Kruger, A. Janshoff, *Biophys. J.* **2004**, *86*, 1545.
[14] H. J. Butt, V. Franz, *Phys. Rev. E: Stat., Nonlinear, Soft Matter Phys.* **2002**, *66*, 031601.
[15] S. Loi, G. Sun, V. Franz, H. J. Butt, *Phys. Rev. E: Stat., Nonlinear, Soft Matter Phys.* **2002**, *66*, 031602.
[16] E. Sackmann, *Science* **1996**, *271*, 43.
[17] R. Tero, *Materials* **2012**, *5*, 2658.
[18] I. Mey, M. Stephan, E. K. Schmitt, M. M. Muller, M. Ben Amar, C. Steinem, A. Janshoff, *J. Am. Chem. Soc.* **2009**, *131*, 7031.
[19] A. Janshoff, C. Steinem, *Biochim. Biophys. Acta* **2015**, *1853*, 2977.
[20] M. Hishida, H. Seto, P. Kaewsaiha, H. Matsuoka, K. Yoshikawa, *Colloids Surf., A* **2006**, *284*, 444.
[21] B. D. Almquist, N. A. Melosh, *Proc. Natl. Acad. Sci. USA* **2010**, *107*, 5815.
[22] B. D. Almquist, N. A. Melosh, *Nano Lett.* **2011**, *11*, 2066.
[23] G. E. Atilla-Gokcumen, E. Muro, J. Relat-Goberna, S. Sasse, A. Bedigian, M. L. Coughlin, S. Garcia-Manyes, U. S. Eggert, *Cell* **2014**, *156*, 428.
[24] M. Yokokawa, K. Takeyasu, S. H. Yoshimura, *J. Microsc.* **2008**, *232*, 82.
[25] M. R. Angle, A. Wang, A. Thomas, A. T. Schaefer, N. A. Melosh, *Biophys. J.* **2014**, *107*, 2091.
[26] L. Redondo-Morata, M. I. Giannotti, F. Sanz, *Langmuir* **2012**, *28*, 6403.
[27] J. M. Fernandez, S. Garcia-Manyes, L. Dougan, *Single Mol. Spectrosc. Chem. Phys. Biol.* **2010**, *96*, 317.
[28] A. F. Oberhauser, P. K. Hansma, M. Carrion-Vazquez, J. M. Fernandez, *Proc. Natl. Acad. Sci. USA* **2001**, *98*, 468.
[29] I. Popa, P. Kosuri, J. Alegre-Cebollada, S. Garcia-Manyes, J. M. Fernandez, *Nat. Protoc.* **2013**, *8*, 1261.
[30] H. Lannon, E. Vanden-Eijnden, J. Brujic, *Biophys. J.* **2012**, *103*, 2215.
[31] S. Garcia-Manyes, J. Brujic, C. L. Badilla, J. M. Fernandez, *Biophys. J.* **2007**, *93*, 2436.
[32] M. Schlierf, H. Li, J. M. Fernandez, *Proc. Natl. Acad. Sci. USA* **2004**, *101*, 7299.
[33] J. Relat-Goberna, S. Garcia-Manyes, *Phys. Rev. Lett.* **2015**, *114*, 258303.
[34] T. Husslein, D. M. Newns, P. C. Pattnaik, Q. F. Zhong, P. B. Moore, M. L. Klein, *J. Chem. Phys.* **1998**, *109*, 2826.
[35] D. Rodriguez-Larrea, H. Bayley, *Nat. Nanotechnol.* **2013**, *8*, 288.
[36] Y. Wu, K. He, S. J. Ludtke, H. W. Huang, *Biophys. J.* **1995**, *68*, 2361.
[37] L. Tayebi, Y. Ma, D. Vashaee, G. Chen, S. K. Sinha, A. N. Parikh, *Nat. Mater.* **2012**, *11*, 1074.
[38] R. M. Sullan, J. K. Li, C. Hao, G. C. Walker, S. Zou, *Biophys. J.* **2010**, *99*, 507.
[39] H. Li, J. M. Fernandez, *J. Mol. Biol.* **2003**, *334*, 75.
[40] G. I. Bell, *Science* **1978**, *200*, 618.
[41] J. Soderlund, L. B. Kiss, G. A. Niklasson, C. G. Granqvist, *Phys. Rev. Lett.* **1998**, *80*, 2386.
[42] C. Park, W. J. Padgett, *Lifetime Data Anal.* **2005**, *11*, 511.
[43] J. L. Folks, R. S. Chhikara, *J. R. Stat. Soc. Ser. B* **1978**, *40*, 263.
[44] I. G. Abidor, V. B. Arakelyan, L. V. Chernomordik, Y. A. Chizmadzhev, V. F. Pastushenko, M. R. Tarasevich, *Bioelectrochem. Bioenerg.* **1979**, *6*, 37.
[45] V. F. Pastushenko, Y. A. Chizmadzhev, V. B. Arakelyan, *Bioelectrochem. Bioenerg.* **1979**, *6*, 53.
[46] W. Weibull, *J. Appl. Mech.-Trans. ASME* **1951**, *18*, 293.
[47] K. Shinoda, W. Shinoda, T. Baba, M. Mikami, *J. Chem. Phys.* **2004**, *121*, 9648.
[48] K. Murzyn, W. Zhao, M. Karttunen, M. Kurdziel, T. Rog, *Biointerphases* **2006**, *1*, 98.
[49] M. Sega, R. Vallauri, S. Melchionna, *Phys. Rev. E: Stat., Nonlinear, Soft Matter Phys.* **2005**, *72*, 041201.
[50] Y. A. Chizmadzhev, F. S. Cohen, A. Shcherbakov, J. Zimmerberg, *Biophys. J.* **1995**, *69*, 2489.
[51] S. Garcia-Manyes, G. Oncins, F. Sanz, *Biophys. J.* **2005**, *89*, 1812.
[52] T. Fukuma, M. J. Higgins, S. P. Jarvis, *Phys. Rev. Lett.* **2007**, *98*, 106101.
[53] K. Shinoda, W. Shinoda, M. Mikami, *Phys. Chem. Chem. Phys.* **2007**, *9*, 643.
[54] S. A. Tristram-Nagle, *Methods Mol. Biol.* **2007**, *400*, 63.
[55] M. Hishida, H. Seto, K. Yoshikawa, *Chem. Phys. Lett.* **2005**, *411*, 267.
[56] M. Hishida, H. Seto, N. L. Yamada, K. Yoshikawa, *Chem. Phys. Lett.* **2008**, *455*, 297.
[57] D. D. Lasic, *Biochem. J.* **1988**, *256*, 1.
[58] A. Schafer, T. Salditt, M. C. Rheinstadter, *Phys. Rev. E* **2008**, *77*, 021905.
[59] E. L. Florin, M. Rief, H. Lehmann, M. Ludwig, C. Dornmair, V. T. Moy, H. E. Gaub, *Biosens. Bioelectron.* **1995**, *10*, 895.

Received: January 12, 2017
Revised: February 17, 2017
Published online:

